3 PF-AR

3-1 Summary

The operation statistics for FY2007 are summarized in Table 1 and the operation time history is shown in Fig. 1. The total operation time in FY2007 was 4561 hours, among which 3614 hours were assigned to users' experiments. The total operation time was somewhat short compared with recent years, since fine adjustments of the new power supply for the bending magnets (described in detail in the last issue of this report) were scheduled in April. The 5% failure rate was considerably larger than in recent years, since it was necessary to suspend operations for several days to take care of problems with the new power supply following the fine adjustments. Excluding the power supply problems the failure rate was 1.3%, comparable to recent years. The power supply problems were caused by harmonics in the power line generated by the new power supply. A filter to suppress the harmonics was installed at the end of FY2007.

The initial beam current of 60 mA and the injection frequency of twice a day were unchanged throughout the year. Operation of the PF-AR was on the whole smooth in FY2007, except for the above-mentioned power supply troubles.

Table 1 Operation statistics of PF-AR in FY2007.

Operation Time	4561.0 h	
SR Experiment	3614.0 h	79.2%
Beam Development	665.0 h	14.6%
Failure	228.5 h	5.0%
Miscellaneous	53.5 h	1.2%

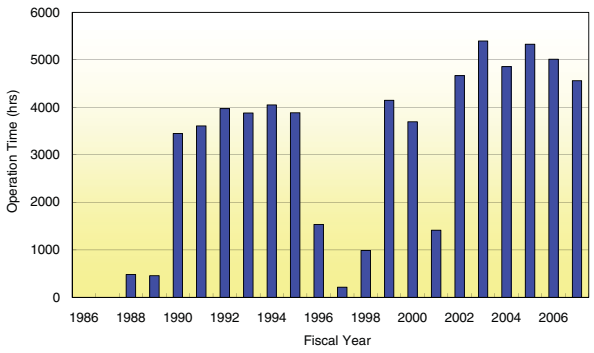

FIgure 1
Operation time history of the PF-AR.

3-2 Movable Synchrotron Radiation Masks with SiC Absorbers

The accelerating system [1] for the PF-AR comprises six 11-cell cavities, two 1-MW klystrons, and RF distribution networks. Two cavities are located in the west straight section and four cavities in the east section. One of the cavities was seriously damaged by synchrotron radiation (SR) in April, 2003 [2], and was replaced with a spare cavity in summer 2004. Though some fixed SR masks were subsequently installed in the cavity sections, they were not enough to block the SR completely. Because each 11-cell cavity for the PF-AR is very long (3.4 m), for an SR mask to protect the cavity from SR it must be located very close to the beam. For most of the upstream cavities (the two cavities in the east and west sections), the head of the mask must be located 19 mm from the beam. Because such a small aperture is not acceptable for beam injection, the SR masks must be movable. Another concern is the high wakefield power generated in the cavity. The PF-AR is routinely operated with single-bunch beams of up to 60 mA, which can induce high parasitic losses in the cavities. Since the SR masks have some trapped resonance modes, beam-induced microwaves from the cavities can build up at the movable masks, damaging the RF contacts. To avoid such problems, the movable masks are equipped with cylindrical microwave absorbers. A schematic view and photograph of the SR mask are shown in Figs. 2 and 3. To manage the high heat density due to the SR (input power: 450 W at 60 mA) from the 6.5-GeV beams, we used an Alumina dispersion-strengthened copper (GlidCop^{TM}) for the mask body. The inside of the mask is water-cooled. The mask can be moved with a stroke of 40 mm using a stepping motor. The microwave absorber, made of silicon-carbide (SiC) is located in the coaxial-line part between the mask head and the RF contactor at the end of the line. The SiC absorber can dissipate the microwave power induced in the neighboring cavity. We carried out high power tests of the movable SR mask in spring 2007. We tested the movable SR mask up to an input power of about 1 kW in the continuous-wave (CW) mode at a frequency of 1.296 GHz. This high power test was quite successful [3], and the masks were installed in the east and west straight sections during the 2007 summer shutdown. Figure 4 shows one of the masks installed in the PF-AR. After testing, the movable SR masks are now routinely operated during beam runs, and are automatically controlled using computer software.

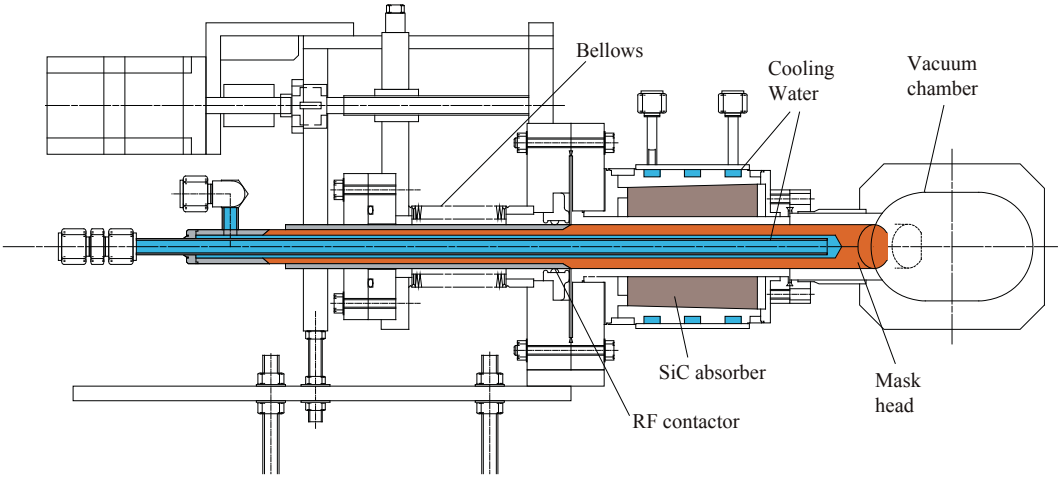

Figure 2
Schematic view of the movable SR mask.

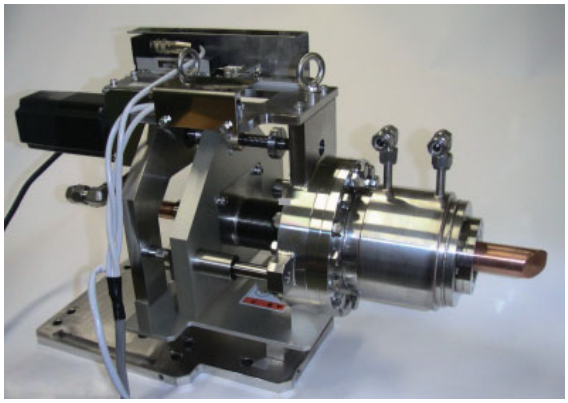

Figure 3
Photograph of the movable SR mask.

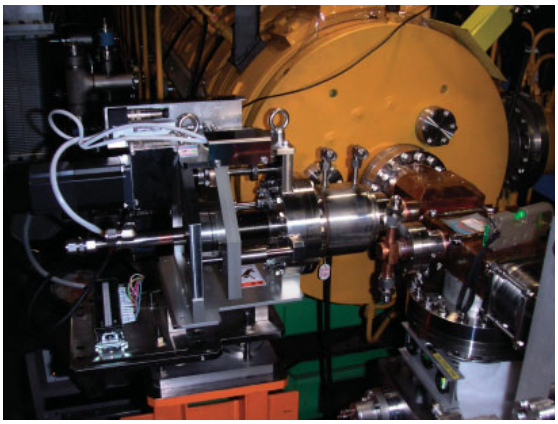

Figure 4
The movable SR mask in the PF-AR.

3-3 Pulsed Quadrupole Magnet Injection

Various attempts have been made to overcome the strong beam instabilities observed during low-energy injection at the Photon Factory Advanced Ring (PF-AR). One attempt was to realize a new injection scheme using a pulsed quadrupole magnet (PQM) with no local bump [1]. This new scheme seemed to be effective, since the PQM did not generate large coherent dipole oscillations. However, we have met much higher barrier than the conventional injection scheme with the dipole kicker magnets.

Figure 5 shows the saturated current of the stored beam as a function of total RF voltage (Vc). A strong dependence was observed for injection using the PQM: while a saturated current of about 60 mA was reached

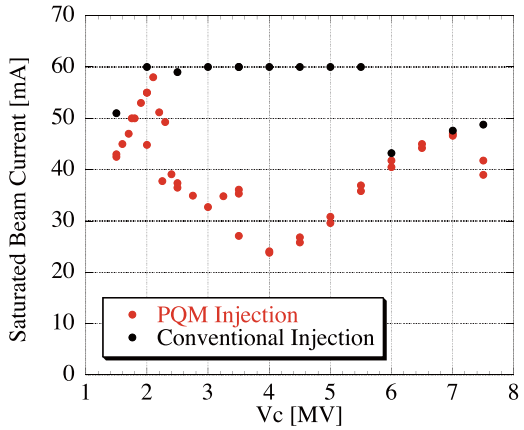

Figure 5
Saturated current of the stored beam as a function of total RF voltage (Vc). The black and red circles represent the beam currents stored using the conventional injection system with a local bump and the new injection system with the PQM, respectively. Because the maximum stored beam current is limited internally to 60 mA by the PF-AR injection system, the plot for conventional injection has a flat region. A strong dependence on total RF voltage was observed for beam injection using the PQM. The injection was carried out at a repetition rate of 12.5 Hz.

REFERENCES

[1] S. Sakanaka, K. Ebihara, E. Ezura, S. Isagawa, T. Kasuga, H. Nakanishi, M. Ono, M. Suetake, T. Takahashi, K. Umemori and S. Yoshimoto, *PAC2003* (2003) 1228.
[2] S. Sakanaka, K. Ebihara, S. Isagawa, M. Izawa, T. Kageyama, T. Kasuga, H. Nakanishi, M. Ono, H. Sakai, T. Takahashi, K. Umemori and S. Yoshimoto, *PAC2005* (2005) 1168.
[3] T. Takahashi M. Izawa, S. Sakanaka and K. Umemori, H. Suzuki, J. Watanabe, *PAC2007* (2007) 248.

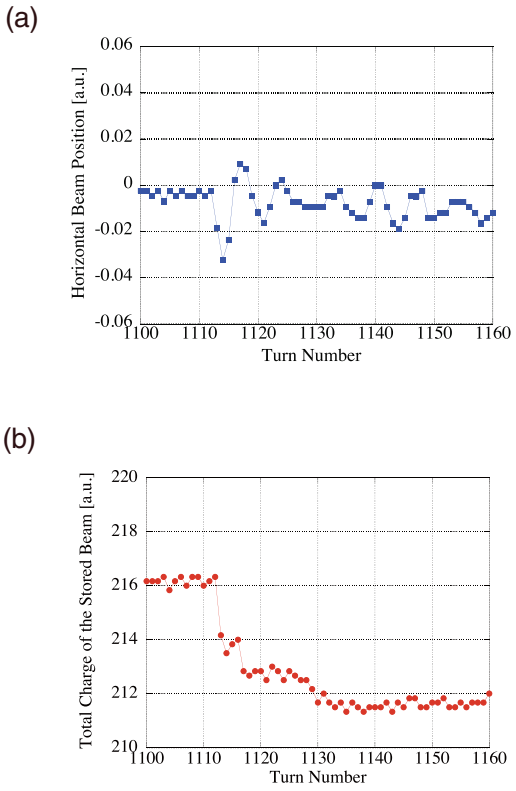

Figure 6
Horizontal position (a) and current (b) of the stored beam as a function of turn number, detected using a turn-by-turn beam position monitor. The excitation timing of the PQM corresponds to the 1112th turn.

at around 2 MV, this decreased to 25 mA at around 4 MV. For the conventional injection scheme in contrast, a saturated current of 60 mA was reached over a wide voltage region, from 2 to 5.5 MV. The behavior of the saturation current of the stored beam in this region is quite different for the two injection methods. To investigate the source of this difference, we conducted several experiments.

Firstly, we examined when the stored beam was lost following excitation of the PQM. We monitored the coherent dipole oscillation and the stored beam current using a turn-by-turn beam position monitor (BPM) with four electrodes. The horizontal dipole oscillation generated by giving a slight offset on the PQM was detected. Figure 6 (a) shows the horizontal beam position as a function of bunch turn number, indicating the excitation timing of the PQM at the 1112th turn. Figure 6 (b) shows the sum of the signals from four electrodes, which corresponds to the stored beam current. In these figures, data is shown from sixty turns, and the vertical axes are arbitrarily scaled. Through these measurements we found out that most of the beam loss occurs within twenty turns following excitation of the PQM. In addition, the growth of the coherent dipole and quadrupole oscillations were not observed until ten thousand turns.

From the timing of the beam loss, we guessed that the extension of the beam size was generated by instabilities having a particular beam current threshold and the beam size was further extended by excitation of the PQM. As a result, part of the beam may be removed by a ring aperture. In addition, the beam loss rate might depend on the extension rate of the beam size, with a consequent strong dependence on the total RF voltage.

To investigate further, we measured the transverse size of the stored beam using a beam scraper during excitation of the PQM. A beam current of 20 mA was initially stored, and then the PQM was excited at a repetition rate of 1 Hz. The beam loss rates were measured as a function of scraper position relative to the beam center, and are shown in Figs. 7 and 8. As the total RF voltages, we chose 2 MV and 4 MV, between which we observed a clear difference in saturated stored beam current, as shown in figure 1. At 2 MV, the full widths calculated from the beam loss rate were 30 mm and 7 mm in the horizontal and vertical directions, respectively. On the other hand, they were 43 mm and 15 mm at a voltage of 4 MV. The horizontal width at 4 MV was about 1.5 times wider than that at 2 MV, and the vertical width was about twice as wide. Moreover, we searched for the location where the beam loss occurred using the local bump method, but were unsuccessful as yet.

Evidence for the extension of the transverse beam profile when the PQM was excited was obtained using the beam scraper. In order to perform a cross check,

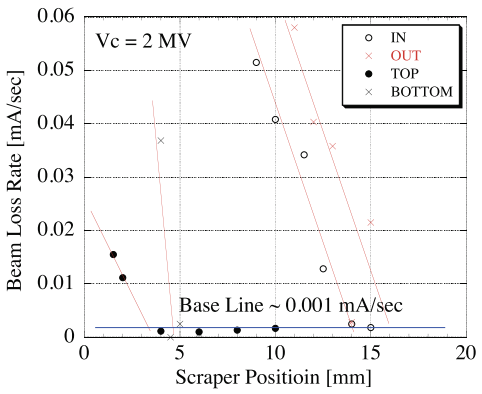

Figure 7
Beam loss rate as a function of scraper position measured at a total rf voltage of 2 MV. The open black circles and the red crosses show the rates measured using the inside and outside scrapers, respectively. The closed black circles and black crosses represent the rates measured using the top-side and bottom-side scrapers, respectively. The solid red lines show the lines fitted by hand. The solid blue line shows the base line of the beam loss rate.

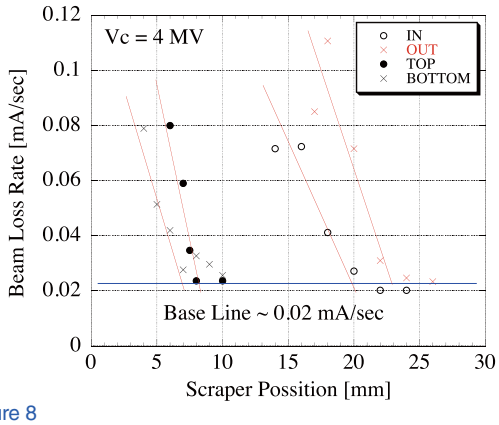

Figure 8
Same as the Fig.3, but measured at a total RF voltage of 4 MV.